

1 **Adenovirus 5 Recovery Using Nanofiber Ion Exchange Adsorbents**

2 Jordan Turnbull,¹ Bernice Wright,¹ Nicola K Green,² Richard Tarrant,² Iwan Roberts,³ Oliver
3 Hardick,³ Daniel G. Bracewell¹

4 ¹Department of Biochemical Engineering, University College London, Bernard Katz
5 Building, Gower Street, London WC1E 6BT, United Kingdom; telephone: +44 20 7679 9580;
6 d.bracewell@ucl.ac.uk

7 ²Clinical BioManufacturing Facility, University of Oxford, Old Road, Headington, Oxford,
8 OX3 7JT, United Kingdom

9 ³Puridify, Stevenage Bioscience Catalyst, SG1 2FX, United Kingdom

10 **Grant Numbers**

11 EP/L01520X/1 and EP/N013395/1

12 **Abstract**

13 Viral vectors such as adenovirus have successful applications in vaccines and gene therapy
14 but the manufacture of high quality virus remains a challenge. It is desirable to use the
15 adsorption based chromatographic separations that so effectively underpin therapeutic protein
16 manufacture. However fundamental differences in the size and stability of this class of
17 product means it is necessary to revisit the design of sorbent's morphology and surface
18 chemistry. In this study, the behaviour of a cellulose nanofiber ion exchange sorbent
19 derivatised with quaternary (Q) amine ligands at defined densities is characterised to address
20 this. This material was selected as it has a large accessible surface area for viral particles and
21 rapid process times.

22 Initially the impact of surface chemistry on infective product recovery using low (440
23 $\mu\text{mol/g}$), medium (750 $\mu\text{mol/g}$) and high (1029 $\mu\text{mol/g}$) ligand densities is studied. At higher
24 densities product stability is reduced, this effect increased with prolonged adsorption
25 durations of 24 minutes with just ~10% loss at low ligand density vs. ~50% at high. This
26 could be mitigated by using a high flowrate to reduce the cycle time to ~1 minute. Next the
27 impact of ligand density on the separation's resolution was evaluated. Key to understanding
28 virus quality is the virus particle: infectious virus particle ratio. It was found this parameter
29 could be manipulated using ligand density and elution strategy. Together this provides a basis
30 for viral vector separations that allows for their typically low titres and labile nature by using
31 high liquid velocity to minimise both load and on-column times while separating key product
32 and process related impurities.

33 **Keywords**

34 Nanofibers, anion exchange chromatography, viral vectors, downstream processing

35 **Introduction**

36 The adenovirus serotype 5 (Ad5) particle is a non-enveloped, icosahedral capsid with a 90-
37 100nm diameter that carries a linear, double-stranded DNA genome (San Martin, 2012).

38 Human Ad5 is the most widely studied adenovirus serotype and is a typical model for viral
39 vector process development (Crystal, 2014). Ad5 is an attractive gene delivery vector due to
40 structural stability, ability to carry large transgene payloads and broad tissue tropism (Crystal,
41 2014). As of 2017, 20% of all gene therapy trials utilise an adenovirus vector (Lee et al.,
42 2017). In the majority of these clinical trials the Ad5 vector fulfils two roles; in an oncolytic
43 capacity for treatment of cancers and as a vaccine whereby the vector expresses a foreign
44 antigenic protein (Keeler, ElMallah, & Flotte, 2017).

45 Downstream processing of viral vectors represents a significant bottleneck and a primary cost
46 of production (Vellinga et al., 2014). Conventionally, industry and academia have relied
47 heavily on the ultracentrifugation technique for downstream purification of highly purified
48 viral vectors (Chen, Marino, & Ho, 2016). However, the process has major drawbacks
49 including poor scalability and high operating costs (Vicente, Roldão, Peixoto, Carrondo, &
50 Alves, 2011).

51 Initial efforts to develop scalable purification platforms led to the repurposing of anion-
52 exchange resins designed for protein purification, building on experience of therapeutic
53 protein processes. Increases in the physical size and complexity of biological products such

54 as viral vectors highlight the limitations of these conventional resin-based chromatographic
55 platforms, for instance poor recovery of the complex biotherapeutics (Lucero et al., 2017).

56 To address this, a number of alternative chromatography materials have been applied to the
57 purification of viruses designed to improve the efficiency and scalability of the process.
58 Monoliths have been applied to Ad5 purification (Whitfield, Batom, Barut, Gilham, & Ball,
59 2009) as well as the separation of much larger enveloped virus species including Vaccinia
60 viruses (350nm) (Vincent et al., 2017). The recovery of a recombinant Ad5 gene therapy was
61 improved from 28% using a Q-Sepharose™ XL column to 35% using a monolith column
62 (CIM™ QA-1) (Lucero et al., 2017). Previous reports showed that the CIM™ QA-1 was
63 preferable over the weak anion CIM™ DEAE-1. The final infective coefficient of virus
64 particle per infective virus particles (VP/IVP) was 13, a range documented as acceptable for
65 potency by the Food and Drug Administration (Kramberger, Urbas, & Štrancar, 2015). Other
66 work using a porous cast membrane Peixoto, Ferreira, Sousa, Carrondo, and Alves (2008)
67 achieved a 62% recovery (determined by cell fluorescence) of infectious Ad5. As well as
68 exploration of alternate adsorbents there has also been a significant amount of work to
69 optimise process and platform design. Piergiuseppe Nestola et al. (2014) described
70 purification of Ad5 using a two column, quasi-continuous, simulated moving-bed size
71 exclusion chromatography (SEC) process which achieved a recovery of 86% determined by
72 real-time PCR.

73 In the this work nanofibers adsorbents are used which have seen a variety of separation
74 applications and can be synthesised in a range of materials such as nylon (Stanelle, M Straut,
75 & Marcus, 2007), glass and cellulose (Ruckenstein & Guo, 2004). The cellulose nanofiber

76 based adsorbents used exhibit a number of physical properties which could be beneficial for
77 Ad5 purification when compared to existing commercial monolith/resin/membranes,
78 including their high surface area and mobile phase accessibility to the entire functionalised
79 surface. Ryu, Kim, Lee, Park, and Lee (2003) reported surface areas of $14 \text{ m}^2\text{g}^{-1}$ for nylon 6
80 nanofibers and poly(4-vinylpyridine) nanofibers were shown to have an area of $26 \text{ m}^2\text{g}^{-1}$
81 (Matsumoto, Wakamatsu, Minagawa, & Tanioka, 2006). Porous cast membranes for
82 bioseparations with a pore size of $0.45\mu\text{m}$ exhibit a surface area of $1\text{-}2 \text{ m}^2\text{g}^{-1}$ a surface
83 significantly lower than nanofibers (Wang, Faber, & Ulbricht, 2009). Beaded porous resins
84 typically have the highest reported surface area at $40 \text{ m}^2\text{g}^{-1}$ (Wen-Chien, Chang-Hung, Ruoh-
85 Chyu, & Keh-Ying, 1995). Despite the high surface area of these resins, the pore size
86 (typically less than 100nm) results in size exclusion of Ad5 from the inner functionalised
87 surface resulting in lower binding capacities (Lusky, 2005) for large biological product such
88 as viruses than would otherwise be expected. The electrospinning process that is used to
89 fabricate the nanofibers requires controlled atmospheric conditions in order to generate
90 consistent nanofiber deposition. Using this approach an average nanofiber diameter within
91 5% of 350nm (Hardick et al., 2011) can be achieved. The fibres are randomly deposited (non-
92 woven) to create a consistent stationary phase architecture to avoid channelling while keeping
93 favourable pressure / flow characteristics (Hardick, Stevens, & Bracewell, 2011). The
94 resulting adsorbent bed once derivatised with an appropriate ligand and packed has convective
95 mass transfer characteristics, and an internal porosity estimated to be 0.62 by mass-density-
96 volume calculations. In this work the nanofibers are packed in a $\sim 0.125 \text{ mL}$ bed, 0.3mm height
97 and 25mm diameter of (Hardick, Dods, Stevens, & Bracewell, 2013).

98 To create nanofibers with the desired separation properties for this use ligand density on the
99 adsorbents is critical. Vicente, Fáber, Alves, Carrondo, and P.B. Mota (2011) demonstrated
100 this parameter impacted recombinant baculovirus (rBV) product quality and impurity
101 clearance for anion exchange membranes. P. Nestola et al. (2014) have shown on similar
102 adsorbents that Ad5 recovery is doubled by reducing the grafted ligand density. In the current
103 study, nanofibers incorporating Q amine ligands at low, medium and high densities on the
104 adsorbent surfaces are used. It is hypothesised that modifying the density of the ligand in this
105 manner would affect Ad5 binding and separation of product and process related impurities,
106 as well as yield.

107 **Materials and Methods**

108 **Materials**

109 The HEK293 cell line used for the generation of Ad5 stocks and for performing the β -
110 galactosidase infectivity titre were purchased from American Tissue Culture Collection
111 (Manassas, VA, USA). Ad5containing a β -galactosidase gene insert were kindly gifted from
112 the Clinical BioManufacturing Facility (Oxford, UK). Nanofiber adsorbents were made to a
113 range of Q amine ligand densities of low (440 $\mu\text{mol/g}$), medium (750 $\mu\text{mol/g}$) and high (1029
114 $\mu\text{mol/g}$) quaternary (Q) ligand density nanofibers by Puridify (now GE Healthcare,
115 Stevenage, UK). All chemicals were purchased from Sigma-Aldrich (Poole, UK) unless
116 otherwise stated. Antibodies for Western blotting analyses were purchased from Abcam or
117 2BScientific. Polyclonal antibody - Primary antibody: Rabbit polyclonal antibody to Ad5
118 (catalogue number: ab6982, Abcam, Cambridge, UK), secondary antibody: Goat polyclonal
119 antibody to rabbit IgG (catalogue number: ab6721, Abcam, Cambridge, UK). Ad5 Hexon

120 antibody - Mouse monoclonal antibody to Ad5 Hexon (catalogue number: 10R-8460
121 2BScientific Limited, Upper Heyford, UK), secondary antibody: Rabbit polyclonal antibody
122 to mouse IgG (catalogue number: ab6728, Abcam, Cambridge, UK).

123 **Methods**

124 **HEK293 Cell Culture**

125 HEK293 cells were cultured in an incubator at 37°C in a 5% (v/v) CO₂ enriched atmosphere
126 at 95% humidity. Cells were cultured for three days and passaged at 80% confluency. Cells
127 were counted using a haemocytometer and they were cultured in Dulbecco's Modified Eagle's
128 Medium from Life Technologies (catalogue no: 21969035, Paisley, UK) supplemented with
129 10% (v/v) foetal bovine serum (Sigma-Aldrich, Steinheim, Germany), 1% (v/v)
130 penicillin/streptomycin (Life Technologies, Paisley, UK), and 2mM L-glutamine (Biochrom,
131 Cambridge, UK). Cells were cultured in 10-tiered HYPERFlasks[®] (Sigma-Aldrich,
132 Steinheim, Germany).

133 **Adenovirus 5 Propagation in HEK293 Cells**

134 Infection of HEK293 cells with Ad5 was performed by adding 100 µL, 5.1 x 10⁹ VP of Ad5
135 in 2.5% glycerol to HYPERFlasks[®] containing HEK293 cells at 80% confluency. The cells
136 were then incubated for 48 h in the cell culture incubator at 37°C, 5% (v/v) CO₂ and 95%
137 humidity.

138 **Adenovirus 5 Harvest and Clarification**

139 To harvest Ad5 propagated in HEK293 cells, the HYPERFlasks[®] were knocked, removing
140 the cells from culture surface, and the contents transferred to 50 mL centrifuge tubes. Cells

141 were stored on dry ice for 30 min and thawed at 37°C for 40 min. The cycle of freezing and
142 thawing was performed three times to disrupt the cell membrane (Lucero et al., 2017). The
143 cell lysate was then centrifuged at 2000 rpm for 10 min, and filtered using 33mm
144 Polyethersulfone (PES) membrane sterile syringe driven filters (0.45µm, Merck Millipore,
145 Feltham, UK) and pooled. Tangential flow filtration (TFF) of the clarified cell lysate was
146 conducted on a KR2i system using a 500kDa molecular weight cut off (MWCO) D06-E500-
147 05-N hollow fiber (length 65cm, surface area 370cm²; both Spectrum Labs, Breda, The
148 Netherlands) at a flow rate of 20 mL/min and transmembrane pressure of 2 Psi (± 0.5). The
149 cell lysate was concentrated 4X and dialysed in binding buffer (20 mM Tris, pH 7.4) 5X
150 volume of retentate, sample was then diluted 1 in 4 to original harvest volume to control for
151 changes in loading volume when comparing TFF and CCL feed.

152 **Scanning Electron Microscopy Analysis of Adenovirus 5 Binding to Quaternary Amine** 153 **Functionalised Nanofibers**

154 Quaternary amine functionalised nanofiber disks were washed with ddH₂O and submerged in
155 an aqueous binding buffer containing 20 mM Tris pH 7.4. The nanofibers were then
156 conditioned in fresh binding buffer for 30 min. Clarified Ad5 (~10⁹ VP: 100 µL) in culture
157 media was added to 900 µL fresh binding buffer to which the discs were submerged and
158 agitated at room temperature for 60 min. A selection from this sample of nanofiber disks were
159 washed in binding buffer to remove non-bound material and submerged in 1% (v/v)
160 glutaraldehyde solution for 10 seconds and left to dry at room temperature. A second batch
161 of nanofiber disks were prepared as before and then submerged in 20 mM Tris, 1 M NaCl pH
162 7.4 for 5 minutes, the nanofibers were then washed with ddH₂O and submerged in 1% (v/v)

163 glutaraldehyde aqueous solution for 10 s and dried at room temperature. Scanning electron
164 microscopy (SEM) was used to image the virus particles bound the adsorbent, the open
165 structure of nanofibers meant that no manipulation of the nanofiber bed was required to
166 visualise adsorbent surface. Nanofibers were mounted on aluminium stubs using adhesive
167 carbon taps. Mounted samples were coated in a 2 nm layer of gold/palladium using a 681
168 Gatan ion beam coater (Roper Industries, Abingdon UK) and imaged using a JEOL 7401
169 FEGSEM (JEOL, Peabody, MA US).

170 **Chromatography**

171 Two different Ad5 containing feeds were assessed to determine if a reduction in process
172 impurities achieved by incorporating a TFF step into the process would change the feed
173 binding characteristics on nanofiber membranes. Two feeds were prepared. One a cell lysate
174 clarified by 33mm Polyethersulfone (PES) membrane sterile syringe driven filters (0.45µm,
175 Merck Millipore, Feltham, UK), referred to as clarified cell lysate (CCL). The second feed
176 was prepared taking CCL then processed using TFF, referred to as 'TFF'. Experiments were
177 performed using an ÄKTA Avant (GE Healthcare Life Sciences, Buckinghamshire UK), with
178 online measurements of pH, conductivity and UV absorbance (260 and 280 nm). The ~0.125
179 mL nanofiber adsorbent (bed height 0.3mm, diameter 25mm) was equilibrated with 10 mL
180 wash buffer containing 20 mM Tris, pH 7.4 at a flow rate of 10 mL/min. 5 mL Ad5 feed at a
181 concentration of $\sim 10^8$ filled virions per mL (VP/mL) was loaded onto the nanofiber adsorbent
182 that was washed with binding buffer until conductivity reached a constant reading. A linear
183 20 mL gradient elution (20 mM Tris, 1 M NaCl, pH 7.4) was applied to nanofibers at a flow

184 rate of 10 mL/min to elute Ad5 bound to the nanofiber adsorbent. The nanofiber adsorbent
185 was washed with 2M NaCl 20 mM Tris, pH 7.4.

186 To investigate the effect of prolonged adsorption durations on Ad5, 5 mL of CCL was loaded
187 onto the nanofiber and wash steps were performed with 10, 40, 80 or 240 mL equilibration
188 buffer at a flow rate of 10 mL/min. Peak resolution was determined by identifying peaks from
189 20 mL gradient elutions and a step elution methodology was developed using the relative salt
190 concentrations identified.

191 The resolution of peaks was refined by extending the gradient elutions when multiple peaks
192 with similar isoelectric points were identified. Total run time for step elution was limited,
193 whilst maintaining a constant flow rate of 10 mL/min, to minimise any potential effects of
194 prolonged adsorption durations on Ad5 infective recovery whilst allowing high resolution
195 separations. Elution fractions were collected using a F9-R fraction collector (GE Healthcare
196 Life Sciences, Buckinghamshire UK). All samples were diluted 1 in 7.5 in phosphate buffered
197 saline to minimise the effects of high salt on recovery of infective Ad5 particles.

198 **Western Blotting**

199 Fractions were concentrated using Vivaspin[®] Turbo 4 (Sartorius, Gottingen Germany). Total
200 protein was quantified using the Modified Lowry protein assay according to manufacturer's
201 instructions (ThermoFischer, East Grinstead, UK). Protein samples were treated 1:1 with
202 Laemmli sample treatment buffer: 50 mM Tris-HCl, 4% (w/v) SDS (Sigma), 10% (v/v) β -
203 mercaptoethanol (Sigma), 20% (v/v) glycerol (Sigma), a trace of Coomassie brilliant blue R
204 (Sigma), pH 6.8, and heated at 95°C for 5 min. Proteins were separated via SDS-PAGE using

205 NuPAGE™ precast 10%, BisTris mini-gels (ThermoFischer, East Grinstead, UK) with gels
206 run at 100V per gel. Proteins were transferred from gels to polyvinylidene difluoride
207 membranes using an iBlot™ 2 gel transfer device following the manufacturer's instructions.
208 Blots were blocked with 5% milk (w/v) for 1 h at room temperature before they were
209 incubated in primary antibody (mouse monoclonal antibody to Ad5 hexon in 2% milk (w/v))
210 overnight at +4°C. Blots were washed three times in 1X tris buffered saline-tween (TBS-T)
211 for 5 min before incubating in secondary antibody (rabbit polyclonal antibody to mouse IgG
212 (HRP-conjugated) in 2% milk) for 2 h at room temperature. Blots were imaged after a 1 min
213 incubation in enhanced chemiluminescent reagent using an Amersham Imager 600 (GE
214 Healthcare Life Sciences, Buckinghamshire UK).

215 **Analysis of Purified Adenovirus 5 using Transmission Electron Microscopy**

216 Transmission electron microscopy was used to visualise Ad5. To perform the analysis, Ad5
217 particles were negatively stained by adding uranyl acetate to Ad5 samples. The stained
218 samples were dropped onto a carbon grid (400 mesh) and loaded onto JEOL 1010
219 Transmission Electron Microscope (JEOL, Peabody, MA USA) before they were imaged.

220 **Host Cell Protein Quantification**

221 Host cell protein (HCP) concentrations from purified Ad5 fractions were analysed using the
222 HEK293 HCP ELISA kit F650R (Cygnus Technologies, Southport, NC, USA) following
223 manufacturer's instructions.

224 **Quantitative PCR**

225 To assess total Ad5 capsids containing DNA, samples were analysed using Adeno-X™ Rapid
226 Titer Kit (Takara Bio Europe, Saint-Germain-en-Laye, France). Briefly, samples were pre-
227 treated with DNAase to remove ex-virus DNA, and then chemically lysed with protease; DNA
228 was isolated using NucleoSpin® Virus Columns (Takara Bio Europe, Saint-Germain-en-
229 Laye, France). Samples were added to master reaction mix in a 96 well plate so that each well
230 contained 2 µL of unknown sample or standard control DNA, 6.8 µL PCR-grade H₂O, 0.4 µL
231 Adeno-X forward primer (10 µM), 0.4 µL Adeno-X reverse primer (10 µM), 0.4 µL ROX™
232 Reference Dye LMP, 10.0 µL SYBR® Advantage qPCR Premix. All reaction were performed
233 using a CFX Connect™ Real-Time PCR Detection System (Applied Biosystems, CA, USA)
234 using the following cycle conditions: stage one, 95°C for 30 seconds; stage two, 95°C for 5
235 seconds, followed by 60°C for 30 seconds (40 repetitions); stage three, dissociation curve of
236 95°C for 10 seconds, 65°C to 95°C increment 0.5°C every 5 seconds. To ensure that
237 recoveries obtained from NucleoSpin® Virus Columns (Takara Bio Europe, Saint-Germain-
238 en-Laye, France) were not affected by the range of salt conditions present in the elution
239 samples, a range of samples containing standard control DNA containing 20 mM Tris, and a
240 range of salt concentrations from 0-0.5 M NaCl (all pH 7.4) were also analysed.

241 **Adenovirus 5 Cell Infectivity Assay**

242 The detection and quantification of Ad5 units that were able to deliver the β-galactosidase
243 gene were analysed as a measure of sample infectivity using the β-galactosidase reporter gene
244 staining kit (Sigma-Aldrich, Taufkirchen Germany). Reactions were conducted following
245 manufacturer's instructions but they were modified for a 96-well plate format. Briefly, plates

246 were coated in poly-L-lysine for 10 min. HEK293 cell suspension of concentration of 4×10^5
247 cells per mL were loaded per well and incubated overnight. Growth media was removed from
248 wells prior to transfection with serial dilutions of Ad5 (100 μ L of Ad5 sample in
249 supplemented DMEM) and the plate incubated for 1h at 37°C. The Ad5 sample was then
250 removed from wells, replaced with 100 μ L of growth media and the plate was incubated
251 overnight at 37°C. To stain, media was removed from wells and cells (attached to well
252 surfaces) were washed twice with phosphate buffered saline (PBS), fixed with 1X fixation
253 buffer (20% formaldehyde, 2% glutaraldehyde in 10X PBS) and incubated for 10 min at room
254 temperature. Wells were washed twice with PBS followed by 30 μ L of staining solution.
255 Plates were incubated at 37°C for 24 h and blue stained cells were manually counted using a
256 light microscope.

257 **Results and Discussion**

258 **Binding and Elution of Adenovirus 5 under Batch Conditions**

259 Batch experiments were conducted to gain insight into the mechanism for virus binding with
260 the purification materials (Wickramasinghe, Carlson, Teske, Hubbuch, & Ulbricht, 2006).
261 Direct imaging of bound virus particles was conducted using scanning electron microscopy
262 (SEM) to determine if the binding and elution interaction behaved as expected using
263 previously described buffer conditions (Peixoto et al., 2008). Adenovirus 5 particles were
264 bound to anion exchange nanofibers under batch conditions by submerging nanofiber disks
265 into binding buffer containing the virus. The nanofibers were then imaged using SEM (Figure
266 1). Adenovirus 5 virions measure ~90nm in diameter and are clearly visible bound to the
267 nanofiber adsorbent. Other host cell components are also visible as a layer bound to the

268 nanofiber surface. To determine if product and impurity components had migrated into the
269 inner bed structure as expected several cross sections through the nanofiber bed were imaged
270 with no observable differences between layers (data not shown). To elute the bound virus,
271 nanofibers were submerged in high salt (1 M NaCl, 20 mM Tris, pH 7.4) elution buffer
272 subsequent SEM reveals all components were visibly removed from the nanofiber surface
273 (Figure 1).

274 **Comparison of Clarified and Buffer Dialysed Adenovirus 5 Feeds**

275 Adenovirus 5 harvest was clarified with 0.45 μ m filters, this clarified cell lysate (CCL) was
276 divided - 50% was further processed using ultrafiltration and diafiltration (UF–DF) with a
277 500kDa TFF system to retain Ad5 and remove bulk host cell impurities before dialysis into
278 binding buffer. The TFF and CCL feeds were analysed using the β -galactosidase infectivity
279 assay to characterise the effect of processing on Ad5 infective potency. After TFF filtration
280 the retentate had an infective recovery of 89% compared to the CCL.

281 A 5 mL ($5.6 \times 10^8 \pm 5.6 \times 10^7$ IVP) volume of CCL Ad5 feed was loaded onto a 0.125 mL
282 anion exchange nanofiber adsorbent at 10 mL/min (Figure 2), and a 20 mL gradient elution
283 of up to 1 M NaCl was applied to the column. The elution profile was then compared to a 5
284 mL ($5.6 \times 10^8 \pm 5.6 \times 10^7$ IVP) load of TFF feed under the same process conditions. This was
285 repeated for low, medium and high density Q amine ligand nanofibers. A large flow through
286 peak was observed for all the ligand densities when challenged with CCL feed. This was not
287 observed for the TFF feed, due to the removal of impurities during the TFF step. The total
288 UV peak area for the TFF feed is reduced compared to the CCL feed, again due to clearance
289 of host cell impurities. Comparison of the CCL feed across the three different Q amine

290 nanofibers (low, medium and high ligand density) shows elution profiles are distinct across
291 all three fiber types (Figure 2), with components binding more tightly giving rise to more
292 peaks and requiring higher ionic strength to elute as ligand density increases. There are more
293 subtle differences seen for the TFF treated material, which are more noticeable at the highest
294 charge density. An explanation could be that with the reduced impurity levels present in the
295 TFF material interactions between Ad5, impurities and the charge surface that allow
296 discrimination for the CCL material are reduced. The distinct elution profile across the three
297 fiber types, demonstrate different separation capabilities of nanofibers as the Q amine ligand
298 density changes. This suggests that by tailoring the ligand functionalisation of the nanofibers
299 it is possible to optimise Ad5 purification process for improved separations.

300 **Extended Adsorption Periods on Quaternary Amine Functionalised Nanofibers Reduce** 301 **Adenovirus 5 Infectivity**

302 Poor viral vector recoveries over an ion exchange chromatography step have been attributed
303 to prolonged adsorption periods that cause degradation of capsid integrity and entrapment of
304 virus particles in the complex internal adsorbent structures (Trilisky & Lenhoff, 2009).
305 Hardick et al. (2013) showed that the large inter-fiber space and morphology of the
306 functionalised surface of nanofibers minimises diffusive mass transfer limitations, a property
307 which has been shown to be detrimental to capacity and recovery of large biotherapeutic
308 molecules (Wickramasinghe et al., 2006). This open structure (Figure 1) may minimise
309 entrapment events and multipoint attachment, suggesting loss in infective units is a result of
310 irreversible binding or capsid damage.

311 The effects of prolonged binding duration on the recovery of infective Ad5 (Figure 3) was
312 analysed. CCL clarified Ad5 feed (5 mL) was loaded onto nanofiber columns and adsorption
313 durations were selected to approximately replicate binding durations of current
314 chromatographic viral vector manufacturing processes. Figure 4 shows overlay
315 chromatograms for low ligand density 1, 4, 8 and 24 min adsorption periods. A 100% recovery
316 of infective virus was observed after the shortest binding duration (1 min) using low ligand
317 density nanofibers (Figure 3). Extending binding durations from 4-24 min using low ligand
318 density nanofibers did not cause a significant decrease in the infectivity of Ad5 eluate, with
319 recoveries between 87-90%. At an extended adsorption duration of 24 min there was a
320 dramatic loss of almost 50% in total infective capsids for medium and high ligand density
321 nanofibers. Significant losses in Ad5 infective recoveries were also observed on high ligand
322 density nanofibers after adsorption periods of 1-8 min and 8-24 min adsorption periods.

323 The substantial losses in Ad5 infectivity observed with use of the medium and high ligand
324 density nanofibers indicates product damage. This could be a result of loss of critical features
325 of the virus for its infectivity, i.e. fiber proteins (McNally, Darling, Farzaneh, Levison, &
326 Slater, 2014). Alternatively the loss of infective units could be caused due to deformation of
327 the capsid as it is 'pulled' onto the functionalised surface over the adsorption duration
328 damaging the capsid. Similar effects have been observed during the recovery of virus-like
329 particles of recombinant hepatitis B virus surface antigen (Huang et al 2006). This is of
330 particular relevance for Ad5 as Perez-Berna et al. (2012) have shown that the virus maturation
331 process gives rise to a metastable structure. These brittle capsids may show a reduced
332 resistance to multipoint attachment, when compared to immature non-infective Ad5. These

333 data suggest that although medium and high ligand density nanofibers limit the recovery of
334 infective Ad5 over extended adsorption periods, acceptable recovery can be achieved if the
335 rapid bind/elute times possible with these nanofiber adsorbents is utilised.

336 **Quaternary Amine Functionalised Nanofibers Achieve Efficient, High Yield** 337 **Purification of Infectious Adenovirus 5 Particles**

338 Vicente, Fáber, et al. (2011) reported that changing ligand density caused a clearer impact on
339 bovine serum albumin (BSA) binding capacity than on both rBV and Ad5. To investigate
340 whether an impact could be seen on Q functionalised nanofibers the same range of three ligand
341 densities were exposed to a greater vector load challenge. Here the nanofiber column volume
342 (CV) 0.125 mL, was loaded with 50 mL (400 CV) TFF processed Ad5 feed (total load $2.39 \times$
343 10^{10} VP, 5.6×10^9 IVP) (Figure 5). Five 10 mL flowthrough fractions were collected from
344 each run and screened for the presence of infective Ad5 capsids. No infective Ad5 capsids
345 were present in the flowthrough (data not shown) which is indicative that capacity was not
346 reached. Based on the SEM image (Figure 1) we performed a Fermi estimate of the capacity
347 for viral particles on this nanofiber adsorbent system. Assuming conservatively 25 viral
348 particles bound per micron of nanofiber and calculating in the region of 5,000 km of nanofiber
349 to be present in a 1 mL packed bed we calculate 1.25×10^{14} VP/mL. The load challenge of
350 1.78×10^{11} VP/mL measured in this study was significantly lower than the calculated capacity
351 of 1.25×10^{14} VP/mL. The calculated capacity for the nanofibers exceeded what we were able
352 to test in this study. In low titre vector manufacturing process the dynamic binding capacity
353 (DBC) would likely not be reached as many 1000s of CVs would be required.

354 *In vivo* therapeutic loads of Ad5 range from 10^8 to 10^{12} virus particles (VP) per dose
355 depending on the therapy and site of administration (Habib et al., 2001; Smaill et al., 2013).
356 Whilst further work to determine the upper limit of capacity is required at the current scale, a
357 single 0.125 mL column can recover ten 10^9 VP doses per cycle. Operating at 10 mL/min
358 (4,800 CV/h), a conservative flowrate for this adsorbent with an 80 mL full cycle, the
359 nanofibers exhibit a productivity of 1.43×10^{15} VP/L/h. In comparison a 1 mL Sepharose Q
360 XL column operating at 0.5 mL/min was shown to have an Ad5 DBC of 1.30×10^{11} VP by
361 Bo et al. (2015) which gives rise to a productivity of 4.88×10^{13} VP/L/h. Under these
362 assumptions nanofibers exhibit a 29-fold increase in productivity compared to conventional
363 packed bed resins.

364 This compares favourably with Hardick, Dods, Stevens, and Bracewell (2015) where it is
365 shown nanofibers are capable of operating at high flow rates to increase protein purification
366 productivity, achieving a 15-fold increase compared to packed bed adsorbents. Running the
367 Ad5 separation at this higher velocity (70 mL/min) shows no significant impact on Ad5
368 infective recovery (data not shown). Operating under these conditions nanofibers could
369 achieve a productivity of 1×10^{16} VP/L/h.

370 **Reproducibility and Life Cycle Performance of Quaternary Amine Functionalised** 371 **Nanofibers**

372 High performance and reproducible performance of chromatography tools are paramount in
373 bioprocessing (Rathore & Sofer, 2005). Nine consecutive bind/elute profiles for each
374 nanofiber ligand density were compared to demonstrate operational reproducibility. There
375 was no detectable loss in binding capacity after nine runs across all three nanofiber ligand

376 densities suggesting a 2M NaCl wash was sufficient to remove TFF Ad5 feed components
377 between runs (data not shown). The absorbance flow profiles were then compared to two
378 more nanofiber cartridges of the same chemistry to demonstrate manufacturing
379 reproducibility. Peak area variability of <5% was observed between cartridges suggesting
380 good manufacturing reproducibility (data not shown).

381 **Separation of Infectious Adenovirus 5 Particles using Quaternary Amine Functionalised** 382 **Nanofibers**

383 High infective product recovery is the primary challenge when purifying a viral vector. It is
384 necessary to assess both the total recovery of Ad5 capsids and their infective potency across
385 each unit operation. In Table I, this data is presented for each of the ligand densities (Figure
386 6). Quantitative PCR analysis was used to determine the recovery of total Ad5 VP. At low
387 ligand density fraction LP4 contained the majority of VPs while at medium ligand density it
388 was MP5 and at high ligand density fraction HP6 was found to contain most of the virus
389 particles. TEM analysis was used confirm presence of Ad5 (Figure 7). This increase in
390 fraction number for VP elution with ligand density is anticipated and reflects the
391 chromatograms seen in Figure 6.

392 Adenovirus 5 particle infectivity was measured by counting β -galactosidase staining in
393 infected cells (Table I). The ratio of viral particles to infective viral particles or units (VP/IVP)
394 is often used as an indicator of product quality. At low ligand density the LP4 fraction
395 contained a ratio of 4.59 VP/IVP, MP5 had 5.12, and HP6 4.00 VP/IVP all are within accepted
396 ranges for clinical use (Kramberger et al., 2015) and despite the different ligand densities
397 presenting unique elution profiles with product eluting at different conductivities, the highest

398 titre peaks (LP4, MP5 and HP6) showed a relatively consistent infective ratio. The highest
399 proportion of packed, non-infective Ad5 capsids were separated in HP7 using high ligand
400 density nanofibers with a coefficient of 16.04 VP/IVP, suggesting clearance of a population
401 of lower quality Ad5. Damaged or immature Ad5, represent important possible product
402 related impurities. Therefore their separation is of particular interest for the manufacture of
403 viral vectors for therapeutic use.

404 Clearance of host cell proteins (HCPs) a process related impurity of primary importance in
405 the manufacture of a therapeutic biological product is documented in Table 1. Removal across
406 the TFF and chromatography step was high with >95% (compared to non-purified Ad5 feed)
407 of HCPs removed.

408 The mass balances of packed, infective Ad5 capsid recovery across all nanofibers ligand
409 densities were similarly high (Table I) especially when compared to other membrane
410 adsorbers (P. Nestola et al., 2014) and monoliths (Lucero et al., 2017) with recoveries of 70%,
411 and 34% respectively

412 **Separation of Free Hexon Capsid Protein**

413 Analysis of capsid recovery provides evidence for the separation of free capsid proteins from
414 assembled virus particles. Hexon is a key component within the Ad5 capsid (see Figure 1) but
415 can also be found in non-assembled forms (Klyushnichenko, Bernier, Kamen, & Harmsen,
416 2001). It has been shown to be immunogenic and represents an important product related
417 impurity (Bradley, Lynch, Iampietro, Borducchi, & Barouch, 2012). A western blot (Figure
418 8) was used to show the distribution of hexon during the separations shown in Figure 6. Hexon

419 was identified in the purified fractions, LP3, LP4, MP5, and HP6, demonstrated to contain
420 packed and infective Ad5 capsids. Hexon is also found in MP3 and HP4 fractions that do not
421 contain infective Ad5 particles and therefore is free hexon protein that is not incorporated into
422 complete capsids. This suggests with medium and high ligand density nanofibers it was
423 possible to isolate free hexon from capsid bound hexon, it is possible at low ligand density
424 free capsid does not bind and goes straight into the flow through. The ability to resolve free
425 hexon from an adenovirus feed using a DEAE-Fractogel anion exchange was also
426 demonstrated by Green et al. (2002), eluting, as shown here at low ionic strength (<25
427 mS/cm).

428 **Conclusions**

429 Nanofibers provide a promising scalable capture platform by which to purify Ad5 from HCP
430 and free hexon, producing an enriched product pool with a high product quality as determined
431 by the VP/IVP ratio. Using medium and high ligand density nanofibers it was possible to
432 achieve a separation of product peaks from a hexon rich peak during salt gradient elution. The
433 Ad5 hexon forms the major building block of the virus capsid (>60%) (Perez-Berna et al.,
434 2012) and non-assembled hexon represents major product impurity due to its antigenic
435 properties. We show that nanofiber materials allow very high infective recoveries of >90%.
436 Critical to this is adsorption time, which when reduced from 24 to 8 min improved recovery
437 from ~50% to >90% and up to 97% for 1 min. The macroporosity, convective mass transfer
438 characteristics and shallow bed height of the nanofibers allows for rapid separations in the
439 manner. Operating under these conditions a 29-fold productivity improvement can be
440 achieved over a classical beaded packed bed resin process. The high recovery achieved across

441 this initial capture step allows for a two or three step chromatography process to readily be
442 considered to meet a given product's specification. The results presented here therefore
443 demonstrate potential clinical utility of this nanofiber adsorbent as a high productivity
444 manufacturing technology for the capture of infective Ad5.

445 **Acknowledgements**

446 This research was supported by the UK Engineering and Physical Sciences Research Council
447 (EPSRC) grant EP/L01520X/1, and Puridify (now part of GE Healthcare), in conjunction with
448 grant EP/N013395/1. We would like to thank Mark Turmaine, for support with electron
449 microscopy.

450 **Conflict of interest**

451 No conflict of interest.

452

453

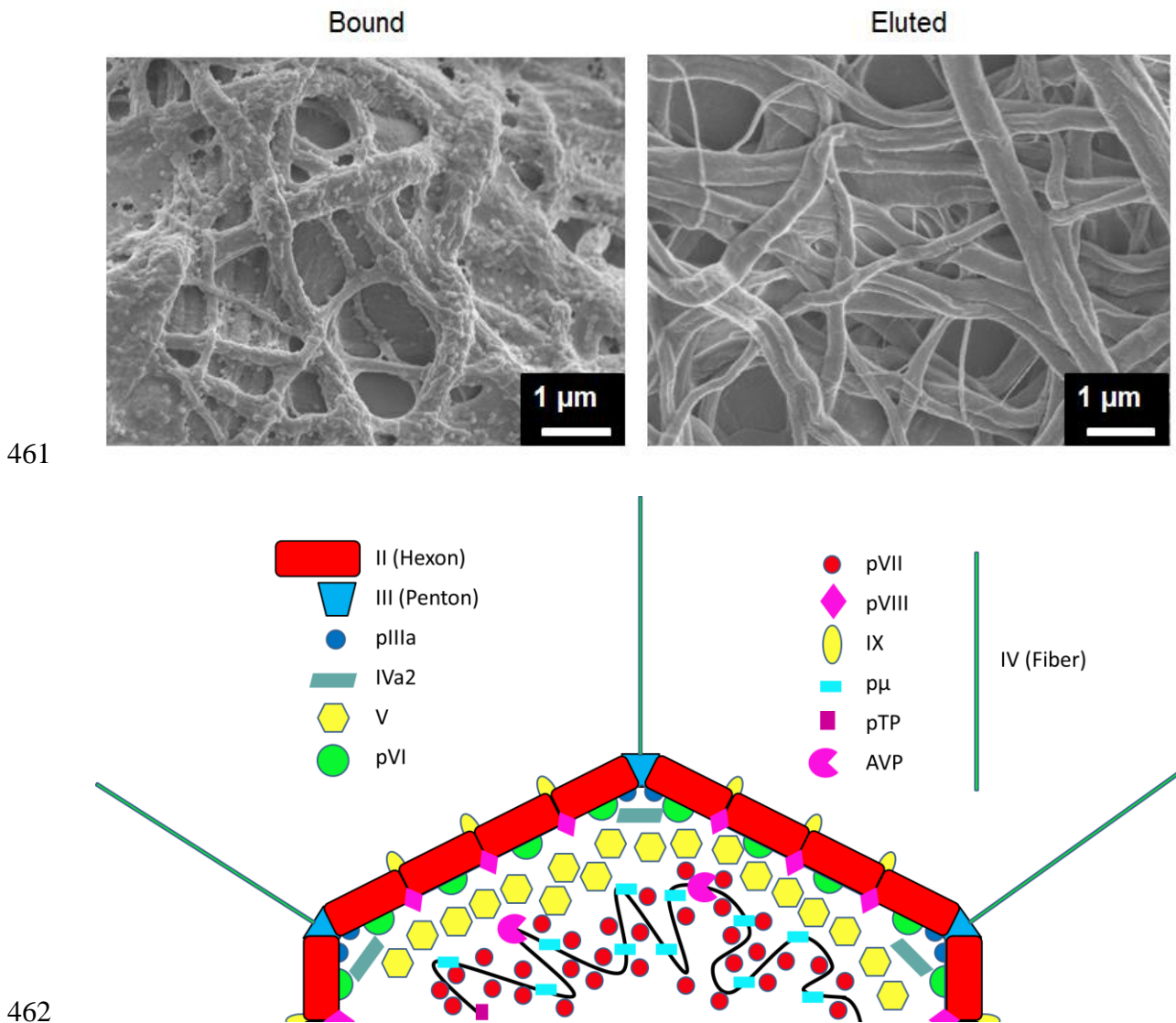
454 **Tables**

455 Table I. The total recoveries of infective Ad5 units (IVP, analysed by β -Gal stain), DNA containing (VP, analysed by qPCR) Ad5 units and the
 456 ratio of these two populations within all Ad5 containing peaks separated on low (440 $\mu\text{mol/g}$), medium (750 $\mu\text{mol/g}$) and high (1029 $\mu\text{mol/g}$) Q
 457 ligand density nanofibers. No qPCR signal was detected for samples LP3 and MP4. Good amounts of host cell protein was shown to be removed
 458 from the Ad5 containing feed, when compared to clarified cell lysate (CCL) Ad5 harvest (1.30E+06 ng/mL) (n=3).

Ad5 containing sample	Sample Volume (mL)	Infectious particle number (IVP)	Standard Error of the Mean	Total IVP Recovery to IVP recovery from TFF	IVP Recovery Standard Error	Virus Particle Number	Standard Error of the Mean	Total VP Recovery to VP recovery from TFF	VP Recovery Standard Error	Infectivity coefficient (VP/IVP)	Eluted NaCl concentration (M)	HCP conc (ng/mL)	Percentage HCP removal from CCL
CCL	Total	6.31E+08	9.40E+06	-	-	-	-	-	-	-	N/A	1.30E+06	0%
Feed (TFF)	Total	5.60E+08	8.70E+06	100.0%	1.53%	2.39E+09	3.30E+07	100.0%	1.31%	4.23	N/A	3.56E+05	72.6%
Low Ligand Density	LP3	8	1.40E+07	4.00E+06		-	-			-	0.29	3.82E+04	97.1%
	LP4	8	4.22E+08	8.72E+06		1.94E+09	5.06E+07			4.59	0.49	4.00E+04	96.9%
	LP5	6	7.13E+07	8.73E+06		3.26E+08	3.03E+07			4.57	1	4.87E+04	96.3%
	Total		5.07E+08		90.2%	2.27E+09		94.8%	3.38%	4.47		4.23E+04	96.8%
Medium Ligand Density	MP4	8	4.20E+07	6.93E+06		-	-			-	0.43	6.28E+04	95.2%
	MP5	8	4.39E+08	1.51E+07		2.25E+09	2.46E+08			5.12	0.6	3.67E+04	97.2%
	MP6	6	3.26E+07	4.99E+06		2.69E+08	3.86E+07			8.25	1	6.05E+04	95.4%
	Total		5.14E+08		91.4%	2.53E+09		105.4%	11.91%	4.93		5.33E+04	95.9%
High Ligand Density	HP6	8	4.97E+08	1.48E+07		1.99E+09	4.71E+07			4.00	0.61	3.32E+04	97.5%
	HP7	6	2.55E+07	5.41E+06		4.09E+08	1.44E+07			16.04	1	5.45E+04	95.8%
	Total		5.23E+08		92.9%	2.40E+09		99.6%	2.57%	4.59		4.39E+04	96.6%

459

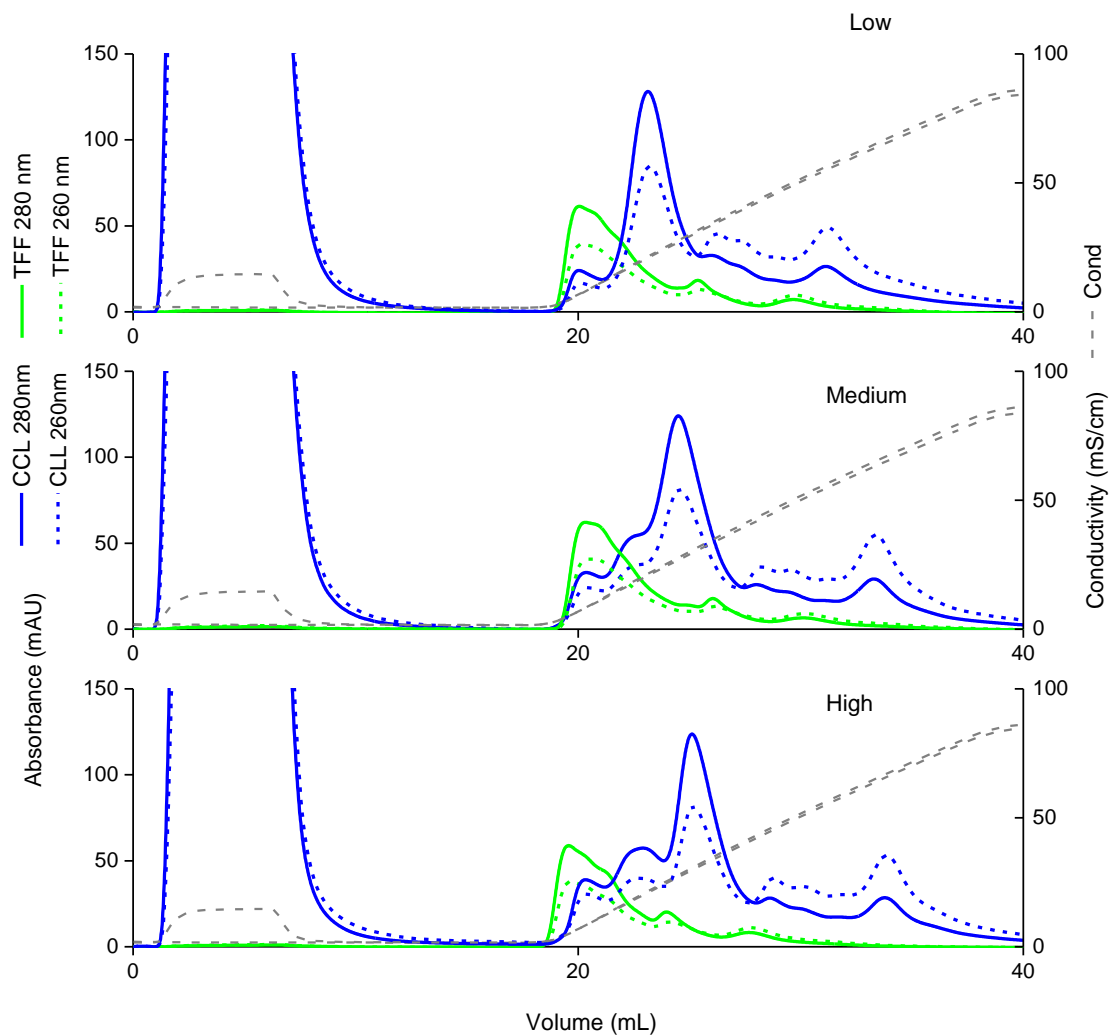
460 **Figures**



463 Figure 1. Top - Scanning electron microscopy images of Ad5 bound to Q ligand and eluted
464 from functionalised nanofibers. Bottom – Diagram of adenovirus proteins, highlighting the
465 level of complexity within each virion (diagram combined from Mangel and San Martin
466 (2014); San Martin (2012)). Adenovirus proteins prefixed with a 'p' denote proteins that
467 undergo proteolysis by adenovirus maturation protein (AVP) as part of a maturation which

468 causes a disassociation of the adenovirus genome from the capsid and a capsid stiffening,
469 priming the capsid for uncoating under endosomal acidification.

470

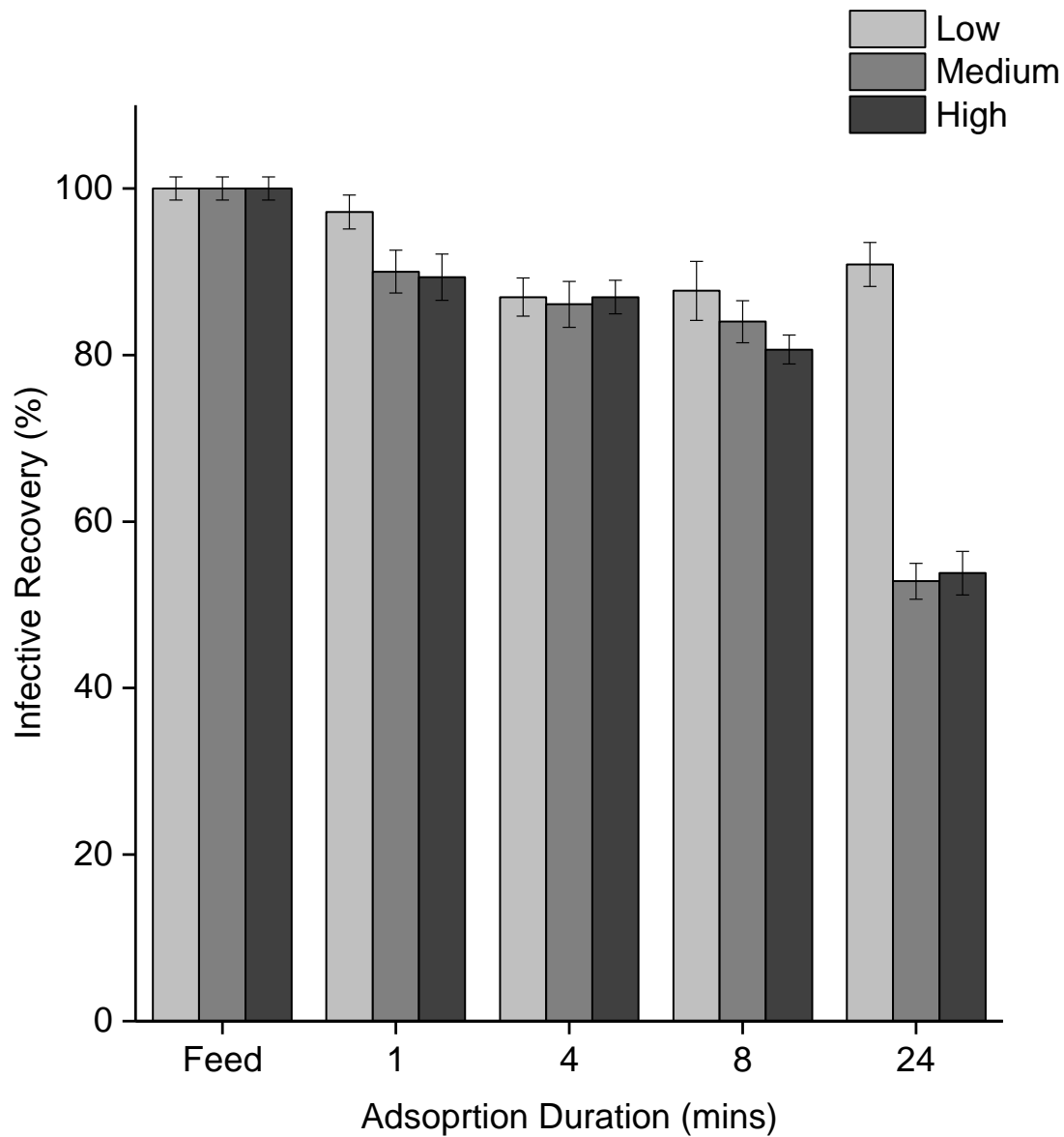


471

472 Figure 2. Elution profile comparison of Ad5 on low (440 $\mu\text{mol/g}$), medium (750 $\mu\text{mol/g}$) and
 473 high (1029 $\mu\text{mol/g}$) Q ligand density nanofibers (CV = 0.125 mL). Ad5 was separated from
 474 a clarified cell lysate (CCL) and a tangential flow filtration (TFF) UF/DF 500 kDa retentate
 475 diafiltered into binding buffer (20 mM Tris, pH 7.4). Loads (5 mL) of both Ad5 feeds
 476 containing a total load of $5.6 \times 10^8 \pm 5.6 \times 10^7$ IVP were used. Chromatograms were generated

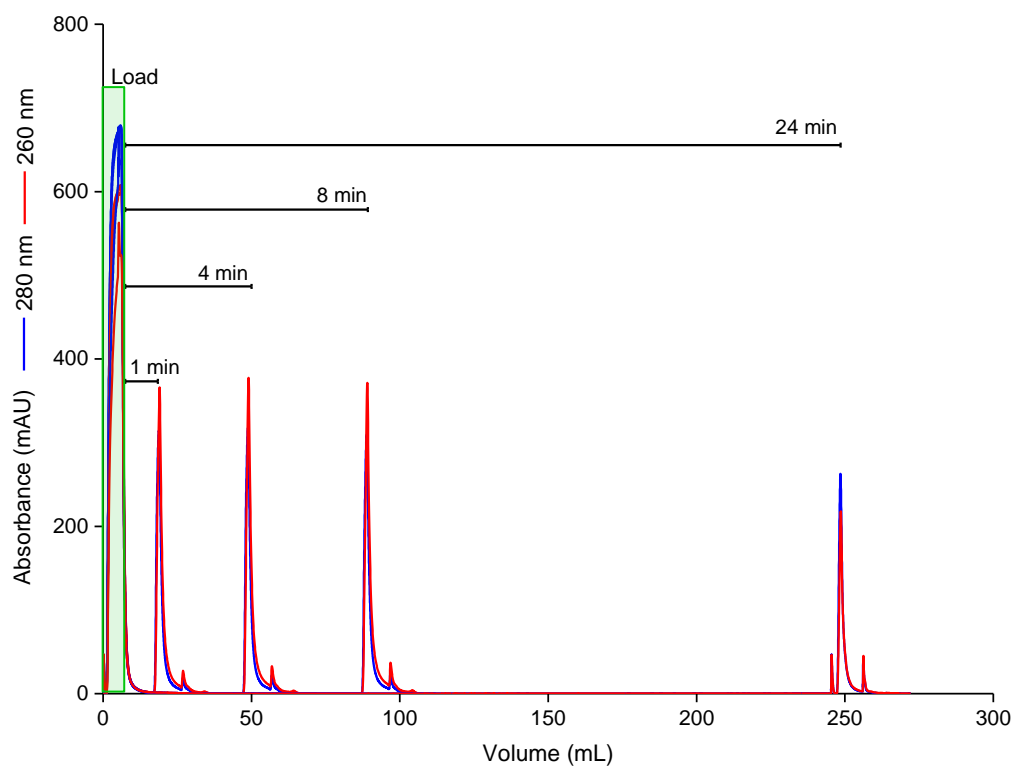
477 using a 20 mL gradient elution at 10 mL/min from 0 M NaCl, 20 mM Tris pH 7.4, to 1 M
478 NaCl, 20 mM Tris pH 7.4 (n=3).

479



480

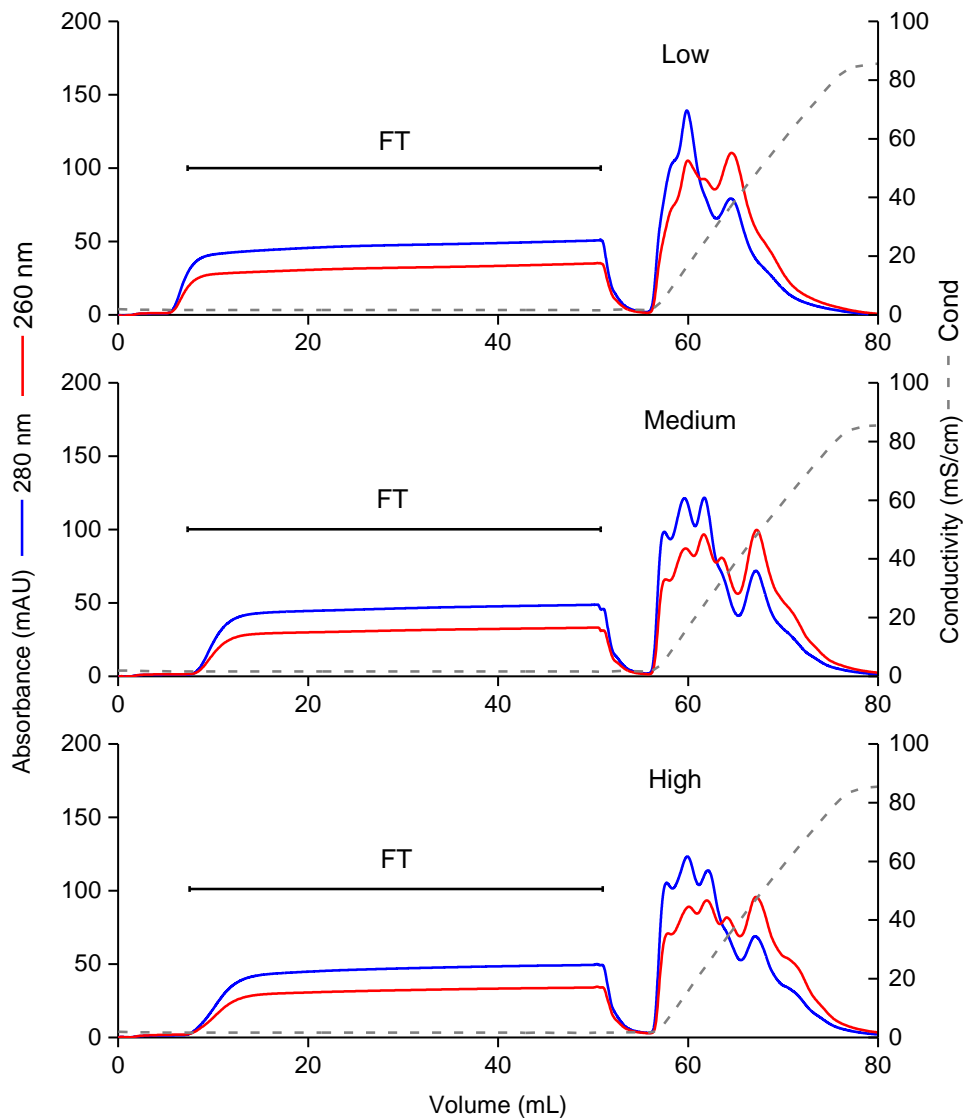
481 Figure 3. Recovery of adenovirus 5 infectivity during adsorption to nanofiber based ion
 482 exchangers, measured by a cell based β -galactosidase reporter assay. Low (440 $\mu\text{mol/g}$),
 483 medium (750 $\mu\text{mol/g}$) and high (1029 $\mu\text{mol/g}$) Q ligand density nanofibers (CV = 0.125 mL)
 484 were loaded with 6.22×10^8 IVP of Ad5 in a clarified feed (n=3).



485

486 Figure 4. Elution profile of four chromatography runs of clarified cell lysate Ad5 feed with
 487 varying wash durations (10, 40, 80, 240 mL or 1, 4, 8, 24 min) in triplicate for a total of twelve
 488 runs for Low (440 $\mu\text{mol/g}$) charge density.

489



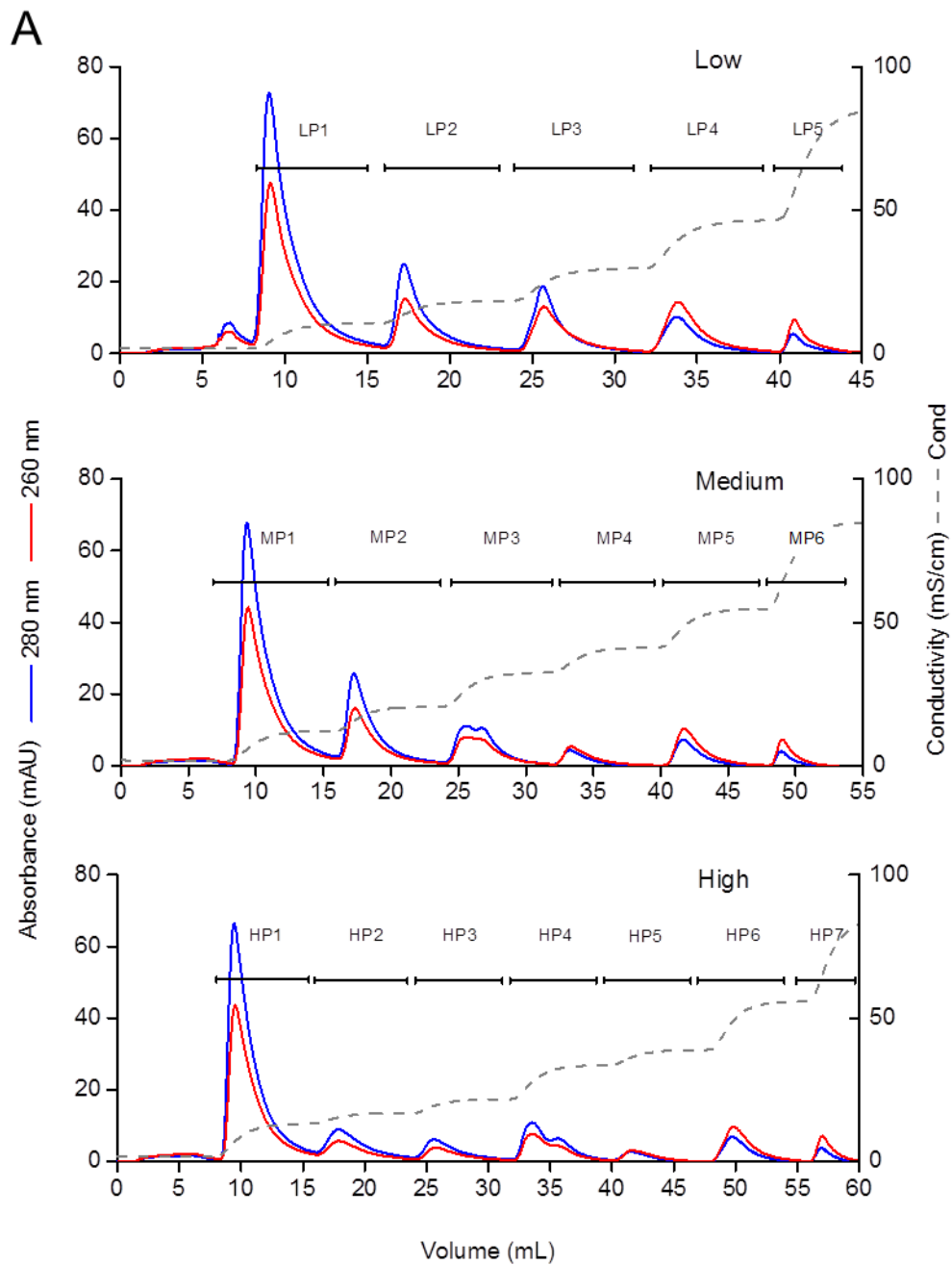
490

491 Figure 5. High loadings of adenovirus feed material to quaternary amine exchange nanofibers.

492 A 50 mL (high volume) TFF Ad5 feed (2.39×10^{10} VP, 5.6×10^9 IVP) was separated using

493 low (440 $\mu\text{mol/g}$), medium (750 $\mu\text{mol/g}$) and high (1029 $\mu\text{mol/g}$) Q amine ligand density
494 nanofibers (CV = 0.125 mL). Fiber saturation was not achieved (n=3).

495

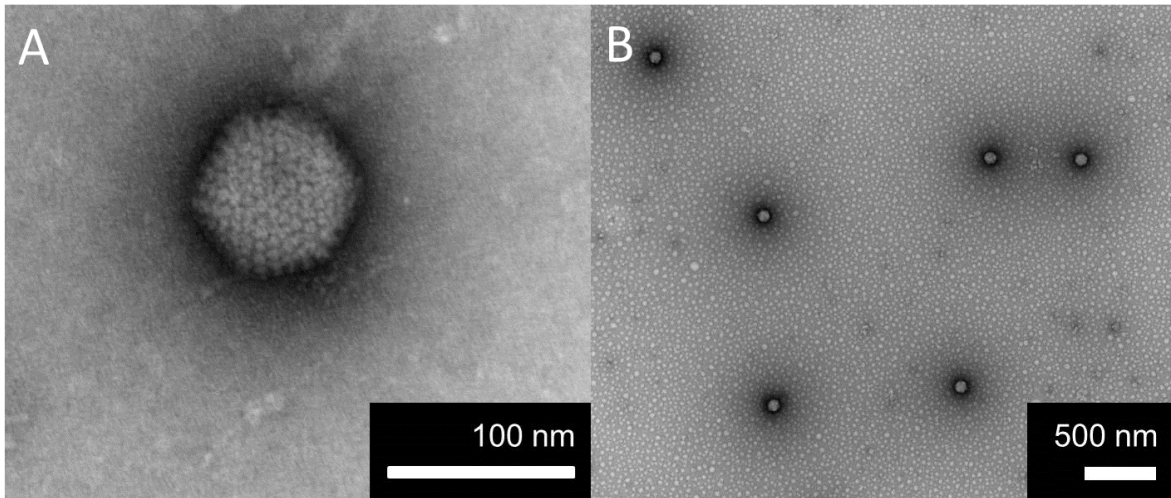


496

497 Figure 6. The impact of increasing Q amine ligand density on the resolution of Ad5 feed
 498 components. Elution peak profiles of low (440 $\mu\text{mol/g}$), medium (750 $\mu\text{mol/g}$) and high (1029
 499 $\mu\text{mol/g}$) Q amine ligand density nanofibers were recorded from a chromatography run of 5

500 mL (2.39×10^9 VP, 5.6×10^8 IVP) TFF feed loaded onto a 0.125 mL nanofiber column at a
501 flow rate of 10 mL/min (n=3).

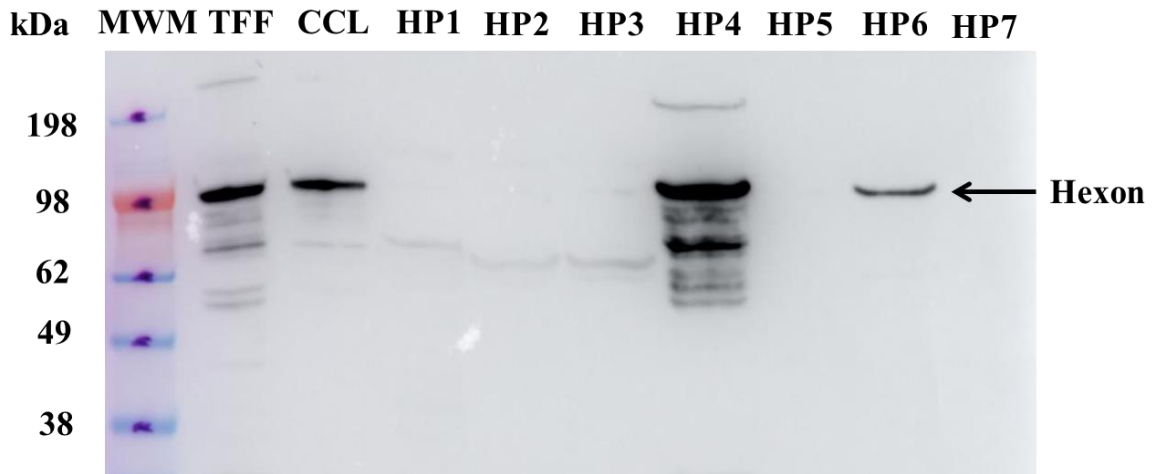
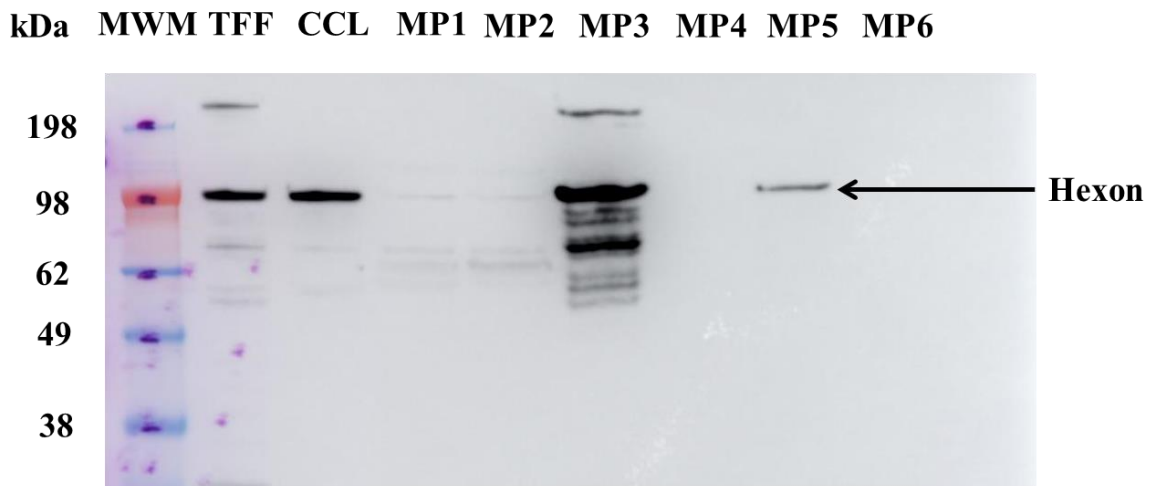
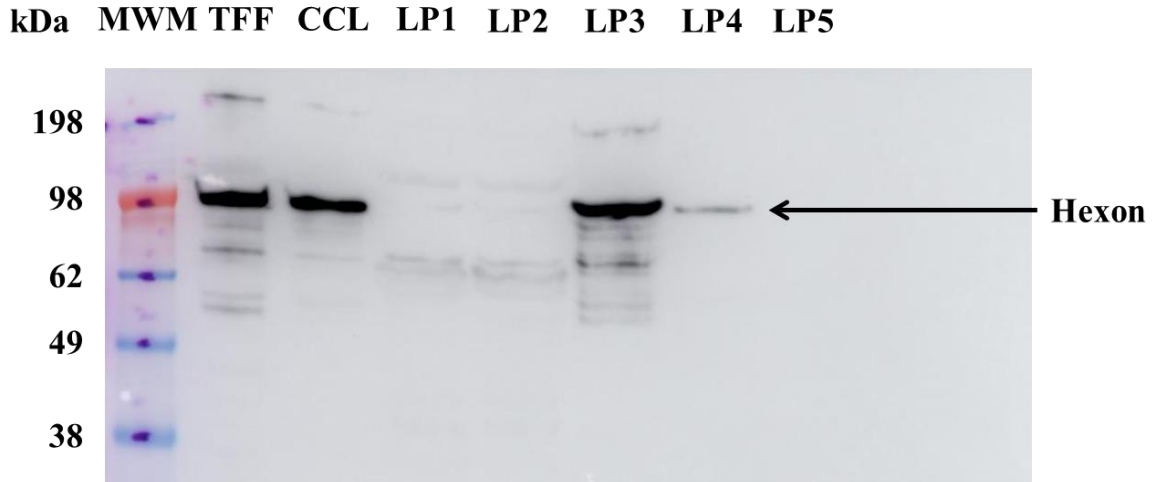
502



503

504 Figure 7. High (A) and Low (B) magnification transmission electron microscopy analysis
505 showed the presence of Ad5 particles in fraction HP6.

506
507



509 Figure 8. Western blot using a Hexon antibody with a secondary antibody (rabbit polyclonal
510 antibody to mouse IgG (HRP-conjugated) showing Adenovirus 5 hexon expression in purified
511 fractions from low (440 $\mu\text{mol/g}$), medium (750 $\mu\text{mol/g}$) and high (1029 $\mu\text{mol/g}$) Q ligand
512 density nanofibers collected from step elution chromatograms (n=3). A molecular weight
513 marker (MWM) and Ad5 from a clarified cell lysate (CCL) and a tangential flow filtration
514 (TFF) UF/DF 500 kDa retentate diafiltered into binding buffer (20 mM Tris, pH 7.4) was also
515 loaded.

516

517 **References**

- 518 Bo, H., Chen, J., Liang, T., Li, S., Shao, H., & Huang, S. (2015). Chromatographic
519 purification of adenoviral vectors on anion-exchange resins. *Eur J Pharm Sci*, *67*, 119-
520 125. doi: 10.1016/j.ejps.2014.11.004
- 521 Bradley, R. R., Lynch, D. M., Iampietro, M. J., Borducchi, E. N., & Barouch, D. H. (2012).
522 Adenovirus serotype 5 neutralizing antibodies target both hexon and fiber following
523 vaccination and natural infection. *Journal of Virology*, *86*(1), 625-629.
- 524 Chen, H., Marino, S., & Ho, C. Y. (2016). 97. Large Scale Purification of AAV with
525 Continuous Flow Ultracentrifugation. *Molecular Therapy*, *24*, S42.
- 526 Crystal, R. G. (2014). Adenovirus: the first effective in vivo gene delivery vector. *Hum Gene*
527 *Ther*, *25*(1), 3-11. doi: 10.1089/hum.2013.2527
- 528 Green, A. P., Huang, J. J., Scott, M. O., Kierstead, T. D., Beaupre, I., Gao, G. P., & Wilson,
529 J. M. (2002). A new scalable method for the purification of recombinant adenovirus
530 vectors. *Hum Gene Ther*, *13*(16), 1921-1934. doi: 10.1089/10430340260355338
- 531 Habib, N. A., Sarraf, C. E., Mitry, R. R., Havlik, R., Nicholls, J., Kelly, M., . . . Salama, H.
532 (2001). E1B-deleted adenovirus (dl 1520) gene therapy for patients with primary and
533 secondary liver tumors. *Human Gene Therapy*, *12*(3), 219-226.
- 534 Hardick, O., Dods, S., Stevens, B., & Bracewell, D. G. (2013). Nanofiber adsorbents for high
535 productivity downstream processing. *Biotechnology and bioengineering*, *110*(4),
536 1119-1128. doi: 10.1002/bit.24765
- 537 Hardick, O., Dods, S., Stevens, B., & Bracewell, D. G. (2015). Nanofiber adsorbents for high
538 productivity continuous downstream processing. *Journal of Biotechnology*, *213*, 74-
539 82. doi: <https://doi.org/10.1016/j.jbiotec.2015.01.031>
- 540 Hardick, O., Stevens, B., & Bracewell, D. (2011). Nanofibre fabrication in a temperature and
541 humidity controlled environment for improved fibre consistency. *Journal of Materials*
542 *Science*, *46*(11), 3890-3898. doi: 10.1007/s10853-011-5310-5
- 543 Huang, Y., Bi, J., Zhou, W., Li, Y., Wang, Y.J., Ma, G., & Su, Z. (2006). *Improving recovery*
544 *of recombinant hepatitis B virus surface antigen by ion-exchange chromatographic supports*
545 *with low ligand density*. *Process Biochemistry* *41* (2006) 2320–2326
546
- 547 Keeler, A. M., ElMallah, M. K., & Flotte, T. R. (2017). Gene therapy 2017: Progress and
548 future directions. *Clinical and Translational Science*.
- 549 Klyushnichenko, V., Bernier, A., Kamen, A., & Harmsen, E. (2001). Improved high-
550 performance liquid chromatographic method in the analysis of adenovirus particles. *J*
551 *Chromatogr B Biomed Sci Appl*, *755*(1-2), 27-36.
- 552 Kramberger, P., Urbas, L., & Štrancar, A. (2015). Downstream processing and
553 chromatography based analytical methods for production of vaccines, gene therapy
554 vectors, and bacteriophages. *Human vaccines & immunotherapeutics*, *11*(4), 1010-
555 1021.
- 556 Lee, C. S., Bishop, E. S., Zhang, R., Yu, X., Farina, E. M., Yan, S., . . . He, T.-C. (2017).
557 Adenovirus-mediated gene delivery: Potential applications for gene and cell-based
558 therapies in the new era of personalized medicine. *Genes & Diseases*, *4*(2), 43-63. doi:
559 <https://doi.org/10.1016/j.gendis.2017.04.001>
- 560 Lucero, A. T., Mercado, S. A., Sánchez, A. C., Contador, C. A., Andrews, B. A., & Asenjo,
561 J. A. (2017). Purification of adenoviral vector serotype 5 for gene therapy against

562 alcoholism using anion exchange chromatography. *Journal of Chemical Technology*
563 *& Biotechnology*, 92(9), 2445-2452. doi: 10.1002/jctb.5255

564 Lusky, M. (2005). Good manufacturing practice production of adenoviral vectors for clinical
565 trials. *Hum Gene Ther*, 16(3), 281-291. doi: 10.1089/hum.2005.16.281

566 Mangel, W. F., & San Martin, C. (2014). Structure, function and dynamics in adenovirus
567 maturation. *Viruses*, 6(11), 4536-4570. doi: 10.3390/v6114536

568 Matsumoto, H., Wakamatsu, Y., Minagawa, M., & Tanioka, A. (2006). Preparation of ion-
569 exchange fiber fabrics by electrospray deposition. *J Colloid Interface Sci*, 293(1), 143-
570 150. doi: 10.1016/j.jcis.2005.06.022

571 McNally, D., Darling, D., Farzaneh, F., Levison, P., & Slater, N. (2014). Optimised
572 concentration and purification of retroviruses using membrane chromatography.
573 *Journal of Chromatography A*, 1340, 24-32.

574 Nestola, P., Silva, R. J., Peixoto, C., Alves, P. M., Carrondo, M. J., & Mota, J. P. (2014).
575 Adenovirus purification by two-column, size-exclusion, simulated countercurrent
576 chromatography. *Journal of Chromatography A*, 1347, 111-121.

577 Nestola, P., Villain, L., Peixoto, C., Martins, D. L., Alves, P. M., Carrondo, M. J., & Mota, J.
578 P. (2014). Impact of grafting on the design of new membrane adsorbers for adenovirus
579 purification. *J Biotechnol*, 181, 1-11. doi: 10.1016/j.jbiotec.2014.04.003

580 Peixoto, C., Ferreira, T. B., Sousa, M. F. Q., Carrondo, M. J. T., & Alves, P. M. (2008).
581 Towards purification of adenoviral vectors based on membrane technology.
582 *Biotechnology Progress*, 24(6), 1290-1296. doi: 10.1002/btpr.25

583 Perez-Berna, A. J., Ortega-Esteban, A., Menendez-Conejero, R., Winkler, D. C., Menendez,
584 M., Steven, A. C., . . . San Martin, C. (2012). The role of capsid maturation on
585 adenovirus priming for sequential uncoating. *J Biol Chem*, 287(37), 31582-31595.
586 doi: 10.1074/jbc.M112.389957

587 Rathore, A., & Sofer, G. (2005). Life span studies for chromatography and filtration media.
588 *Process Validation in Manufacturing of Biopharmaceuticals*, 169-204.

589 Ruckenstein, E., & Guo, W. (2004). Cellulose and glass fiber affinity membranes for the
590 chromatographic separation of biomolecules. *Biotechnol Prog*, 20(1), 13-25. doi:
591 10.1021/bp030055f

592 Ryu, Y. J., Kim, H. Y., Lee, K. H., Park, H. C., & Lee, D. R. (2003). Transport properties of
593 electrospun nylon 6 nonwoven mats. *European Polymer Journal*, 39(9), 1883-1889.
594 doi: https://doi.org/10.1016/S0014-3057(03)00096-X

595 San Martin, C. (2012). Latest insights on adenovirus structure and assembly. *Viruses*, 4(5).
596 doi: 10.3390/v4050847

597 Smail, F., Jeyanathan, M., Smieja, M., Medina, M. F., Thantrige-Don, N., Zganiacz, A., . .
598 . Puri, L. (2013). A human type 5 adenovirus-based tuberculosis vaccine induces
599 robust T cell responses in humans despite preexisting anti-adenovirus immunity.
600 *Science translational medicine*, 5(205), 205ra134-205ra134.

601 Stanelle, R., M Straut, C., & Marcus, R. (2007). *Nylon-6 Capillary-Channeled Polymer*
602 *Fibers as a Stationary Phase for the Mixed-Mode Ion Exchange/Reversed-Phase*
603 *Chromatography Separation of Proteins* (Vol. 45).

604 Trilisky, E. I., & Lenhoff, A. M. (2009). Flow-dependent entrapment of large bioparticles in
605 porous process media. *Biotechnology and bioengineering*, 104(1), 127-133. doi:
606 10.1002/bit.22370

- 607 Vellinga, J., Smith, J. P., Lipiec, A., Majhen, D., Lemckert, A., van Ooij, M., . . . Havenga,
608 M. (2014). Challenges in manufacturing adenoviral vectors for global vaccine product
609 deployment. *Hum Gene Ther*, 25(4), 318-327. doi: 10.1089/hum.2014.007
- 610 Vicente, T., Fáber, R., Alves, P., Carrondo, M., & P.B. Mota, J. (2011). *Impact of Ligand*
611 *Density on the Optimization of Ion-Exchange Membrane Chromatography for Viral*
612 *Vector Purification* (Vol. 108).INCOMPLETE REFERENCE
- 613 Vicente, T., Roldão, A., Peixoto, C., Carrondo, M. J. T., & Alves, P. M. (2011). Large-scale
614 production and purification of VLP-based vaccines. *Journal of Invertebrate*
615 *Pathology*, 107, Supplement(0), S42-S48. doi:
616 <http://dx.doi.org/10.1016/j.jip.2011.05.004>
- 617 Vincent, D., Kramberger, P., Hudej, R., Štrancar, A., Wang, Y., Zhou, Y., & Velayudhan, A.
618 (2017). The development of a monolith-based purification process for Orthopoxvirus
619 vaccinia virus Lister strain. *Journal of Chromatography A*. doi:
620 <https://doi.org/10.1016/j.chroma.2017.09.003>
- 621 Wang, J., Faber, R., & Ulbricht, M. (2009). Influence of pore structure and architecture of
622 photo-grafted functional layers on separation performance of cellulose-based
623 macroporous membrane adsorbers. *J Chromatogr A*, 1216(37), 6490-6501. doi:
624 10.1016/j.chroma.2009.07.042
- 625 Wen-Chien, L., Chang-Hung, L., Ruoh-Chyu, R., & Keh-Ying, H. (1995). High-performance
626 affinity chromatography of proteins on non-porous polystyrene beads. *Journal of*
627 *Chromatography A*, 704(2), 307-314. doi: [https://doi.org/10.1016/0021-](https://doi.org/10.1016/0021-9673(95)00267-Q)
628 9673(95)00267-Q
- 629 Whitfield, R. J., Battom, S. E., Barut, M., Gilham, D. E., & Ball, P. D. (2009). Rapid high-
630 performance liquid chromatographic analysis of adenovirus type 5 particles with a
631 prototype anion-exchange analytical monolith column. *Journal of Chromatography*
632 *A*, 1216(13), 2725-2729. doi: 10.1016/j.chroma.2008.11.010
- 633 Wickramasinghe, S. R., Carlson, J. O., Teske, C., Hubbuch, J., & Ulbricht, M. (2006).
634 Characterizing solute binding to macroporous ion exchange membrane adsorbers
635 using confocal laser scanning microscopy. *Journal of Membrane Science*, 281(1-2),
636 609-618. doi: DOI 10.1016/j.memsci.2006.04.032
- 637

638